

Transcranial Doppler Embolus Detection: A Primer

Emma M. L. Chung

Department of Medical Physics, University Hospitals of Leicester, Leicester, UK

Blood clots and pieces of plaque can detach from the insides of arteries and move to the brain with devastating consequences. In this primer, I describe how this process of embolization can be detected by harnessing the Physics of transcranial Doppler ultrasound.

Keywords: Cerebral emboli, transcranial Doppler ultrasound

Introduction

Solid emboli are formed as a result of 'furring up' of the arteries, and typically consist of thrombus, hard calcified plaque or soft fatty atheroma. Gaseous emboli may also enter the circulation during surgery or form internally from gases that are normally dissolved in the blood. Any foreign body (solid or gas) that becomes free-floating in the blood-stream is called an embolus, from the Greek '*embolōs*' meaning 'a stopper'.

Embolization of plaque and thrombus is a major cause of stroke and is projected to be the world's leading killer by 2020.¹ 'Plugging-up' of the arteries by emboli causes poor oxygen supply to brain tissue (cerebral ischaemia), which can lead to irreversible neuronal damage and cell death (infarction).

Embolus detection using transcranial Doppler (TCD) offers a unique, non-invasive glimpse of the dynamic mechanisms and interactions underlying embolic stroke.² Studies of embolization show that the majority of emboli cause no ill effects, subtle transient symptoms and minor injuries to brain tissue, which can often go unnoticed.

There is a complex relationship between embolization and the brain's ability to protect itself from ischaemia by regulating the blood supply. Even in the event of a major embolic obstruction our arteries provide us with numerous alternative routes to allow blood to get to where it's needed (collateral circulation). The anatomy of the brain and topology of the arteries are also important; an equally severe stroke can arise from obstruction of a small artery supplying a critical area as from a larger blockage. Finally, properties of the blood can play an important role in governing the ability of the brain to clear emboli and the extent to which embolic blockages may cause damage to the artery walls.

Monitoring of patients using TCD can provide warning signs of embolization and an opportunity for clinicians to 'steer' patients out of danger (e.g. by surgically removing plaque or providing medication). TCD monitoring permits detection and early treatment of patients at high risk. It also provides a valuable means of assessing technological advances and pharmacological intervention for reducing embolization.^{3,4}

Doppler Ultrasound

Ultrasonic detection of emboli is based on the Doppler effect proposed by Christian Andreas Doppler in 1842.⁵ Doppler thought that a wave would have a higher frequency if the source was moving toward the observer and a lower frequency if moving away from the observer. The difference between the transmitted (f_t) and observed (f_o) frequencies is called the Doppler shift (f_D), eqn 1:

$$f_D = f_o - f_t$$

The Doppler effect was proved for sound waves by Christophorus Henricus Diedericus Buys Ballot in 1845,⁶ who asked a group of musicians to play a calibrated note from a train on the Utrecht to Amsterdam train line. Musicians on the station platform were asked to listen for the change in pitch (Fig. 1).

Doppler's theory makes it possible to determine the velocity (v) of an object by measuring its Doppler shift (f_D). Since most objects don't emit sound, the Doppler shift is usually measured by detecting changes in the frequency of reflected sound waves. For sound reflected from a moving object, the Doppler shift is doubled and the velocity of the object is given by eqn 2:

$$v = \frac{f_D c}{2f_t \cos \theta_D}$$

The measured velocity depends on the frequency of the transmitted sound (f_t), the local speed of sound (c), and the direction of motion in relation to the observer, as given by the Doppler angle (θ_D). If the source is moving directly toward the observer ($\theta_D=0^\circ$) the Doppler shift will be a maximum. Perpendicular to the source ($\theta_D=90^\circ$) there is no Doppler shift

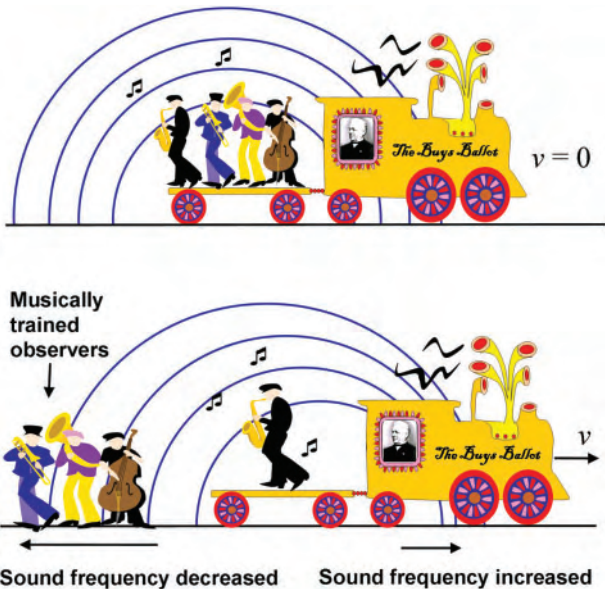


Figure 1. The Doppler effect, first demonstrated by Buys Ballot.⁶

Correspondence: Dr Emma M. L. Chung, Department of Medical Physics, Leicester Royal Infirmary, Leicester, LE1 5WW, UK. emma.chung@uhl-tr.nhs.uk

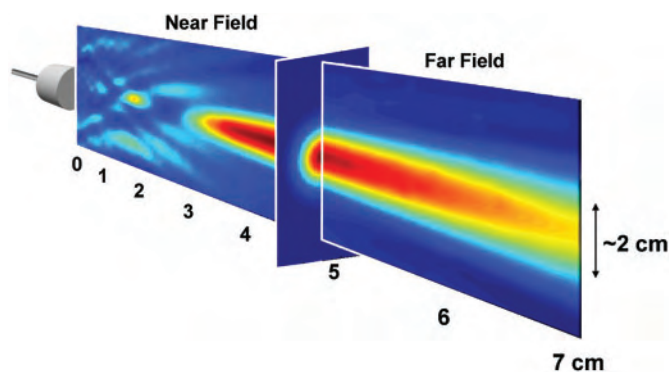


Figure 2. Longitudinal and transverse cross-sections of a typical TCD beam.

at all. If the source is moving away from the observer ($\theta_D=180^\circ$) the Doppler shift will be negative.

The Ultrasound Beam

Ultrasound is generated using a piezoelectric transducer, which changes thickness when an oscillating voltage is applied. The amplitude and frequency of the electrical oscillation is chosen to give the desired amplitude and frequency of ultrasound. When the transducer expands and contracts it moves neighbouring molecules forward and back, creating multiple sound waves. These are focused by a concave outer surface or an acoustic lens to form the ultrasound beam. A typical ultrasound beam used for transcranial Doppler is shown in Fig. 2. The characteristics of the beam depend on the dimensions of the transducer, the ultrasound frequency and the properties of the lens.

Insonation of an Artery

To perform TCD monitoring, the transducer is used to create an ultrasound pulse of $\sim 10\ \mu\text{s}$ duration and $f_t \sim 2\ \text{MHz}$. Pulses are repeated at between 4 and 12 thousand times per second. This is called the pulse repetition frequency (PRF). Following the transmission of a pulse, the transducer starts to receive echoes, which are converted back into an electrical signal called the 'radio frequency' or *RF* signal. This contains frequencies that differ slightly from those of the emitted pulse because of the Doppler effect.

Ultrasound scattered from a chosen depth (sample volume) can be captured by only accepting echoes that arrive at a certain time after transmission (Fig. 3). This is done by

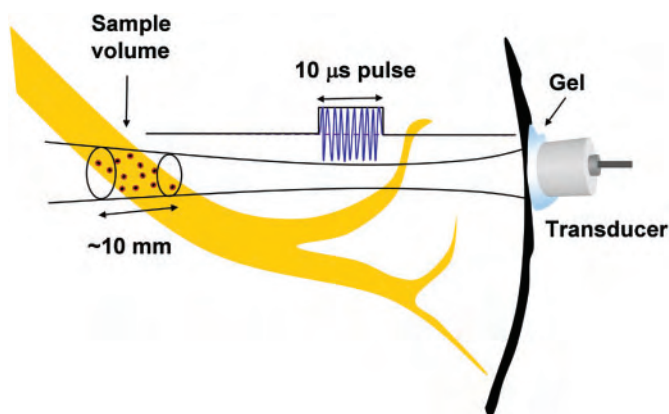


Figure 3. TCD insonation of an artery.

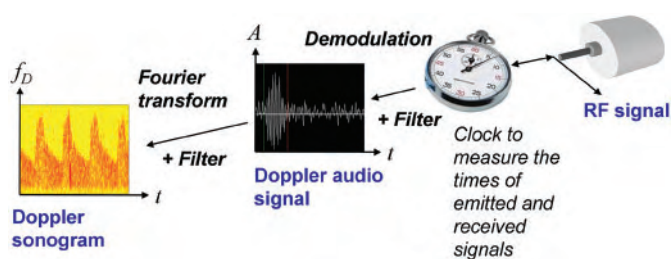


Figure 4. TCD post-processing.

allowing a 'gate' to briefly open (the 'receive gate'). While the gate is open, we 'catch' and analyse the returned echoes.

Processing the Returned Signal

Computerized instrumentation situated between the transducer and the display makes thousands of calculations a second (Fig. 4). The first of these is to separate the Doppler audio signal from the *RF* signal by a process called demodulation.⁷

Demodulation

Demodulation involves 'mixing' or multiplying together the emitted and received signals. The low frequency (Doppler shift) component of the signal is then extracted by 'filtering out' the high frequency components.

Fourier transformation

The audio signal resembles a cacophony of 'whooshing' noise containing Doppler frequencies from the motion of all the scatterers in the sample volume mixed together. To disentangle the different Doppler shift frequencies, we need a way of separating the signal into its original components. Fourier's theorem states that any complex waveform can be built from adding together a series of sine and cosine waves (Fig. 5).

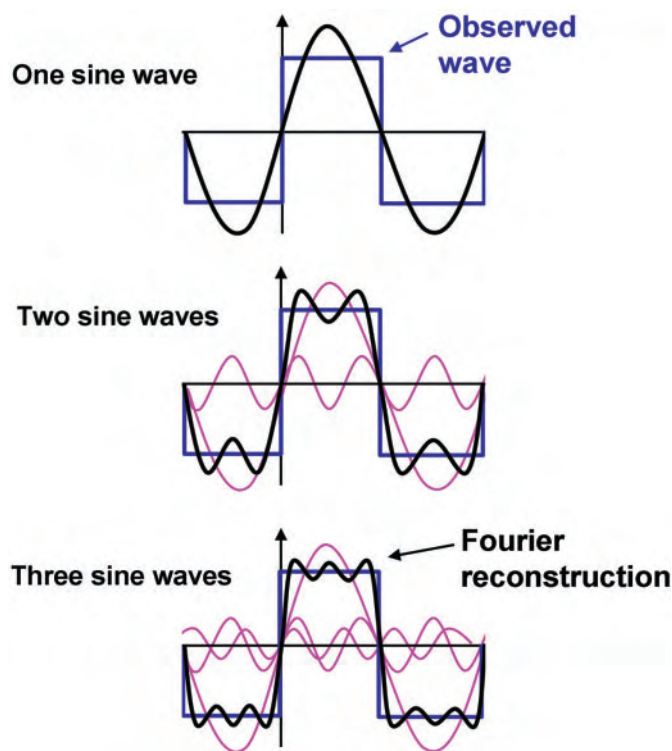


Figure 5. Basic principle of Fourier series.

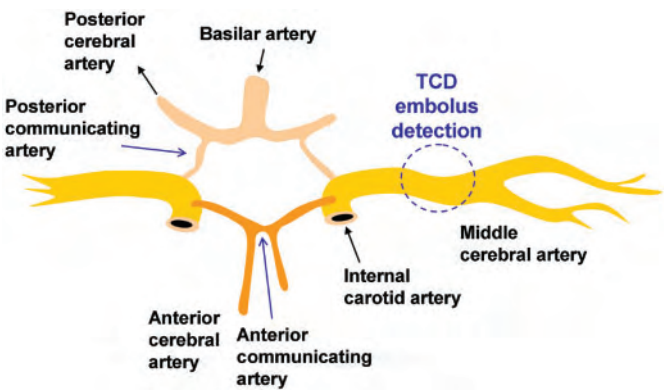


Figure 6. The Circle of Willis.

The waves have different frequencies, amplitudes, and phases, so that they reinforce and cancel one another to reproduce the observed signal.

The Fourier transform is calculated after splitting the audio signal into overlapping 4–10-ms time segments. The distribution of frequencies in each segment is displayed with time as a Doppler sonogram (Fig. 6). The sonogram colour scale shows how much ultrasound of a particular Doppler shift frequency was received. If the Doppler angle between the beam and the direction of flow is known, these frequencies can be converted to velocities using eqn 2.

Most back-scattered ultrasound comes from stationary or slow-moving tissue. Due to their low velocities, this very intense signal occurs at low frequencies and is normally removed by ‘filtering out’ Doppler shift frequencies of less than ~ 100 Hz.

Artefacts

The sonogram often contains strange signals that are not due to the motion of blood or emboli. These artefacts typically arise from the patient’s movements (such as coughing, snoring or talking) or from motion of the TCD probe. If a signal is very intense, the circuitry may become overloaded. This ‘saturates’ the Doppler audio output and produces sharp spikes in the sonogram across a broad range of frequencies.

Another artefact is ‘aliasing’, which appears as a folding of high frequency parts of the spectrum onto lower frequencies. If there were a movie of Buys Ballot’s experiment, it might appear that the train was moving forwards, but the wheels were turning backward. This curious effect occurs because the sampling frequency of film (at 24 frames/s) is too slow to capture the motion of the rapidly rotating wheels. This is known as aliasing. Aliasing can be avoided by checking that the pulse repetition frequency is over twice the maximum Doppler shift frequency from blood flow.

Scattering from Blood

The major cerebral arteries form a pentagon shape called ‘the circle of Willis’ (Fig. 6). To detect emboli, we usually insonate the middle cerebral artery (MCA) by directing an ultrasound beam through a thin region of bone above the ear (the temporal window). The MCA supplies blood to a large region of the brain, and extends horizontally towards the ear. Any emboli arriving from the heart or the carotid artery are likely to enter the MCA where they can be observed using transcranial Doppler.

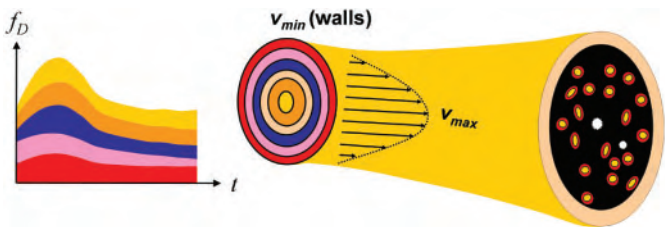


Figure 7. Blood-flow velocities are fastest in the centre of the artery and slowest near the artery walls.

If you were able to travel with the blood, you would see a swirl of red-blood cells (erythrocytes) moving fastest at the centre of the artery and slowest near the walls. The plasma contains a few white blood cells (leucocytes) and many tiny platelets, but most ultrasound that contributes to the sonogram has been scattered by erythrocytes.

The sonogram from blood flow displays a continuous distribution of frequencies, which rises and falls with every heartbeat. The maximum frequency comes from the fastest scatterers in the centre of the artery, and lowest frequencies from blood cells near the artery wall (Fig. 7).

Rayleigh scattering

Each red-blood cell has a diameter of $d \sim 0.008$ mm, which is point-like compared with the $\lambda = 0.78$ mm wavelength of 2 MHz ultrasound moving through blood.

By virtue of being very small ($d \ll \lambda$), blood cells and small emboli scatter ultrasound uniformly in all directions. This is called Rayleigh scattering (Fig. 8).⁸ Lord Rayleigh found that the intensity of scattering was proportional to $d^6 f^4$ (eqn 3):

$$I \propto d^6 f^4$$

Interference between ultrasound scattered from erythrocytes produces varying regions of high and low intensity in the sonogram called the speckle. The appearance of blood flow in the sonogram also depends crucially on the Doppler angle. Frequency shifts will be positive if blood is moving toward the probe and negative if moving away from the probe (Fig. 9). In most TCD machines, the Doppler angle is assumed to be $\theta_D = 0^\circ$, so velocities may actually be higher than displayed. During insonation of the MCA, the average Doppler angle is around $\theta_D = 30^\circ$.⁹

Scattering from Emboli

The intensity of an embolic signal depends on the shape, size and composition of the embolus, its trajectory and the level of

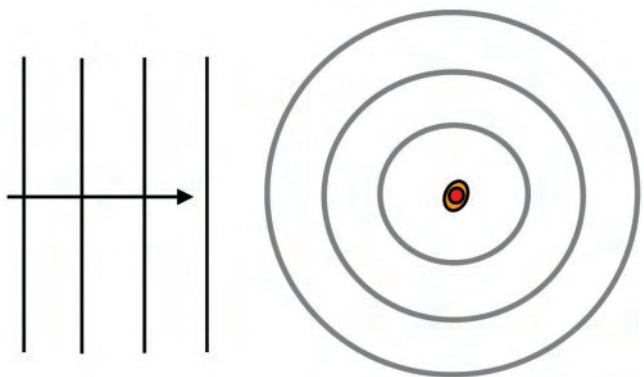


Figure 8. If particles are small in relation to the wavelength of incident ultrasound, the sound will be scattered evenly in all directions (Rayleigh scattering).⁸

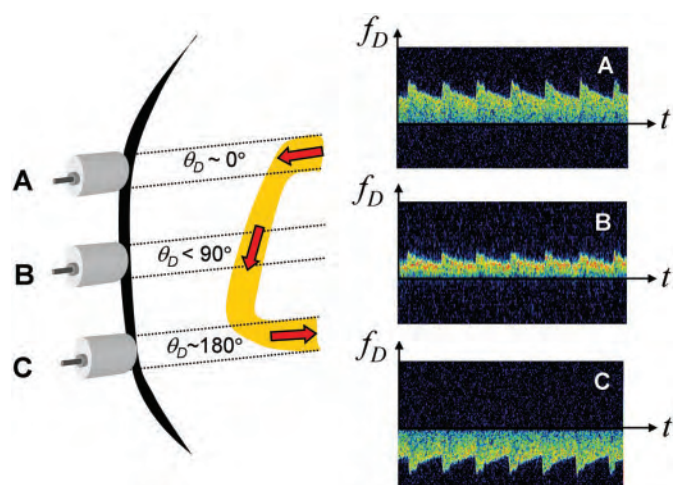


Figure 9. Appearance of blood-flow in the sonogram depends on Doppler angle.

insonation by the beam. The audio signal (sometimes called the time domain signal) often resembles an 'amplitude-modulated sine wave' (Fig. 10, top panel). An embolus travelling at a single velocity produces a brief pure-tone audio signal. This corresponds (via Fourier's theory) to a localized range of frequencies in the sonogram (Fig. 10, bottom panel). If the Doppler angle is known, the velocity of the embolus can be estimated. Changes in speed and trajectory of the embolus cause the frequency of the embolic signal to vary (frequency modulation).

Embolic signals usually last for just a fraction of a second (<100 ms). The faster the embolus passes through the sample volume, the shorter the duration of the signal will be.¹⁰ The sample length and duration of the signal is also longer for stronger scatterers (eqn 4):

$$\text{Duration} \propto \frac{\text{effective sample length}}{\text{velocity}}$$

Measured Embolus-to-Blood Ratio

Motion of an embolus through the sample volume creates a brief increase in the intensity of backscattered ultrasound,

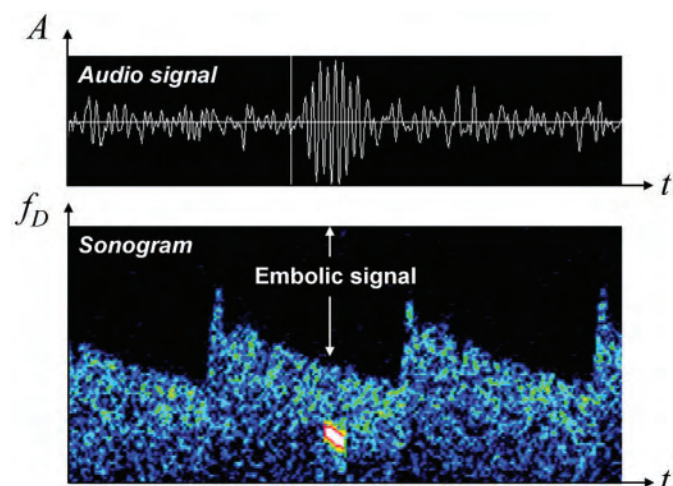


Figure 10. Appearance of a Doppler embolic signal in the audio (time-domain) signal (top panel) and the sonogram (bottom panel). As the embolus enters and exits the sample volume, the intensity of scattered ultrasound rises and falls. The frequency of the signal is proportional to embolus velocity.

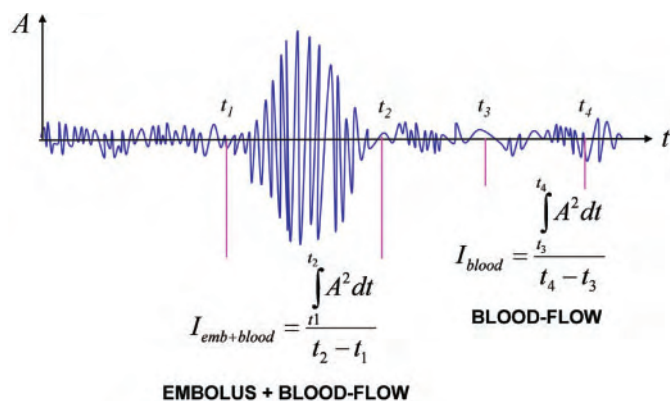


Figure 11. Calculation of MEBr from the audio signal.

which appears brighter in the sonogram than the surrounding speckle. In the audio signal, the Doppler shift sounds like a 'snap', 'chirp' or 'moan'.¹¹ The increase in intensity due to passage of the embolus is measured relative to the average scattering from surrounding blood and is called the measured embolus-to-blood ratio (MEBR).¹² The 'log' converts the ratio to a decibel (dB) scale (eqn 5):

$$MEBR = 10 \log_{10} \left(\frac{I_{emb+blood}}{I_{blood}} \right)$$

MEBR is normally estimated directly from the audio signal (Fig. 12). The intensity of the audio signal is given by the square of its amplitude (A, eqn 6):

$$I = A^2$$

MEBR can be estimated by dividing either the maximum or average intensity of the embolic signal by the intensity of the background blood flow. The average scattering from blood is usually estimated from 'windows' of audio data collected before and/or after the position of the embolic signal (Fig. 12). Values obtained for the MEBR depend on the duration and position of the windows chosen for calculating the average intensities.

Theoretical Embolus-to-Blood Ratio

The theoretical intensity of ultrasound scattered by the embolus, relative to that of the surrounding blood, is called the theoretical embolus-to-blood ratio (EBR, eqn 7).¹³ The scattering cross-sections of the blood (σ_B) and embolus (σ_E) give a measure of scattering strength:

$$EBR = \frac{\sigma_B + \sigma_E}{\sigma_B}$$

By assuming spherical deformable particles, we can predict EBR values for emboli of different densities and sizes (Fig. 12).¹⁴

In general, gas bubbles scatter more ultrasound than fat or thrombus of the same size due to a greater difference in acoustic impedance. However, a single EBR value may correspond to several sizes and compositions of emboli. This makes it difficult to determine embolus size and composition just by measuring an EBR. The relationship between embolic signal intensity and embolus size is also predicted to oscillate due to resonance effects. Particles and bubbles of different sizes have frequencies at which they naturally tend to vibrate. When the frequency of ultrasound

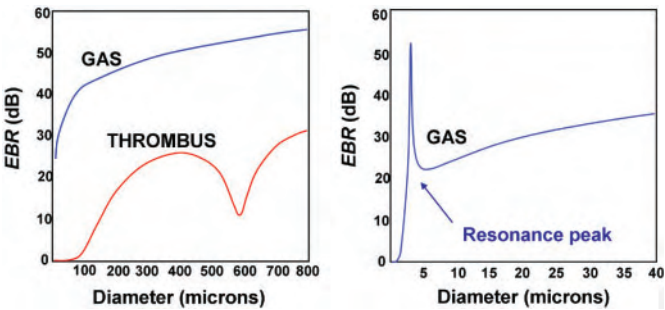


Figure 12. Theoretical predictions for the relationship between embolus diameter and *EBR* for gaseous emboli and thrombus. Calculations were performed by assuming spherical elastic particles insonated by a 2-MHz ultrasound beam (sample volume length=10 mm, vessel diameter=3 mm, haematocrit=45%).¹⁴ A sharp increase in intensity is observed for diameters of emboli with frequencies of vibration matching the frequency of incident ultrasound.¹⁴

matches the natural frequency of the particle, its radius oscillates. This produces a strong peak in the returned scattering (Fig. 12).

Embolic Signals in Clinical Practice

During widening of blocked arteries by angioplasty, surgical removal of plaque, and cardiac surgery, the brain is vulnerable to being showered with thousands of tiny emboli. For example, the stroke risk during open-heart surgery is 3–9%.¹⁵ Filtration devices can be inserted to prevent large emboli from entering the circulation, but whether small micro-emboli (<100 μ m) are really benign is not known. Blockage of tiny arterioles may cause widespread minor infarctions that are too small to be observed by MRI. Gas bubbles are not thought to be harmful provided that the emboli are small, exposure is transitory, and the gases are easily dissolved back into the bloodstream.¹⁶

In clinical practice, strong deviations from theoretical predictions for embolus properties are expected. Emboli have sizes approaching the wavelength of the incident beam, and are irregularly shaped, which makes their scattering patterns erratic (Fig. 13). The ultrasound beam-shape is also severely distorted by the skull. This causes variations in the intensity of insonation and direction of backscatter.¹⁷

Carotid surgery

One common application of TCD embolus detection is for monitoring patients during the surgical removal of carotid plaque. Following carotid surgery, around 3% of patients have several-hundred embolic signals, originating mainly from formation of blood clots at the site of the incision. Embolic

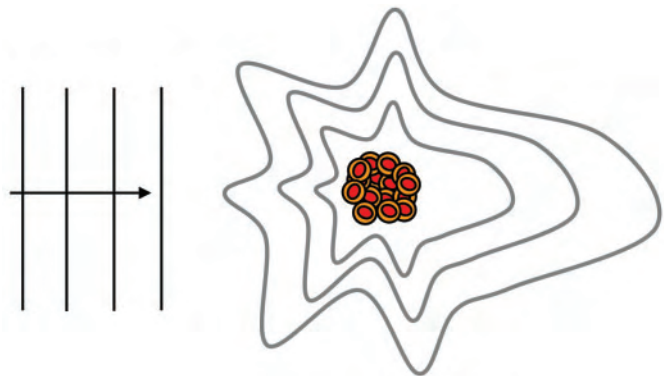


Figure 13. Emboli with sizes approaching the wavelength of incident ultrasound ($\lambda=0.77$ mm) do not scatter ultrasound uniformly.

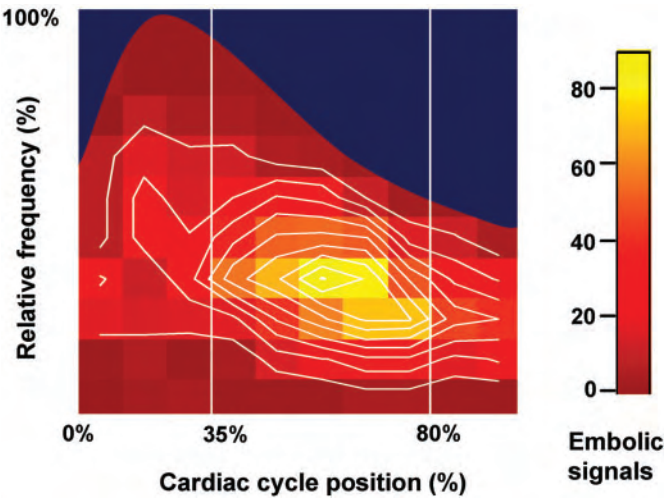


Figure 14. Embolic signals detected following carotid surgery are more likely to be observed between 35% and 80% from the start of systole than elsewhere.¹⁸

signals from fresh thrombus are usually detected at similar positions in the cardiac cycle, due to a strong tendency for pieces of growing thrombus to detach during systole when forces on the walls of the artery are at their greatest (Fig. 14).¹⁸

Following carotid surgery, around 1% of patients have at least one large embolus that barely manages to squeeze through the ~ 2.5 mm diameter of the MCA (Fig. 15). These emboli (known as 'flow-modulating' emboli) cause a temporary disruption of blood-flow, and usually have *MEBRs* of ~ 35 dB. Patients with large emboli, or a high rate of embolization following surgery, are often given drugs to thin the blood and reduce clotting. These patients normally make a full recovery, since emboli from fresh thrombus are easily dissolved and respond well to medication.

Surveys of signal characteristics show that solid emboli produce a narrow distribution of intensities and durations centred on an *MEBR* of ~ 7 dB, and duration of ~ 12 ms (based on a 10-mm nominal sample length) (Fig. 16). Comparison with theory suggests that around 60% of emboli observed following carotid surgery are less than 0.2 mm in diameter. Only 2% of emboli are estimated to be wider than 0.8 mm in diameter.¹⁸ It is also found that signal duration is inversely proportional to frequency. This makes sense because 'faster' emboli spend less time in the Doppler sample volume.¹⁸

Gaseous emboli

Doppler signals from gas bubbles can be characterized by monitoring patients with sources of predominantly gaseous emboli.¹⁹ Rapid decompression or sudden warming of patients during surgery cause gases that are normally dissolved in the blood to form bubbles. This can lead to decompression sickness

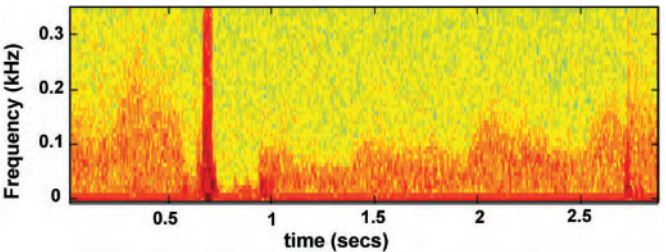


Figure 15. Embolic signal from a 'flow-modulating' embolus. This signal was observed approximately 2 h following carotid surgery during routine monitoring of the MCA.¹⁸

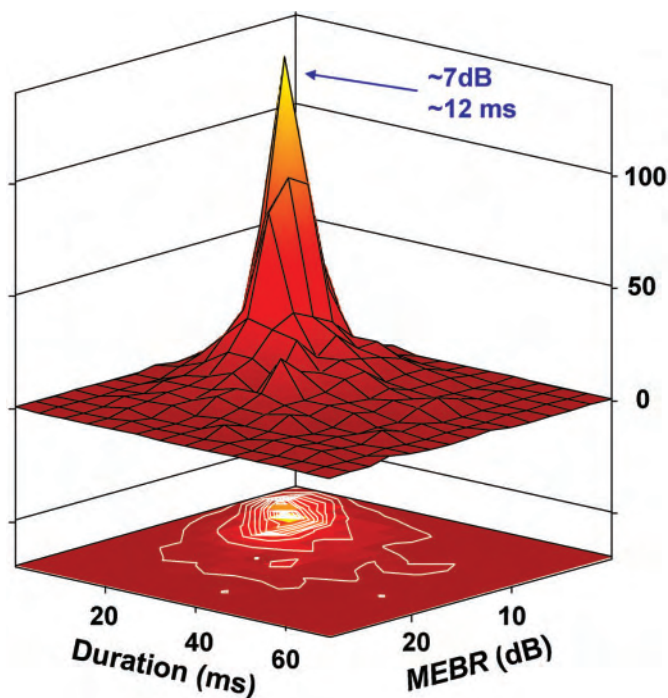


Figure 16. Signals from solid emboli exhibit a characteristic distribution of intensities and durations centred on an MEBR of ~7 dB, and duration of ~12 ms.¹⁸

(the bends).¹⁹ Any invasive surgical procedure also has potential to allow air into the circulation, especially open-heart surgery.¹⁹ Finally, mechanical heart-valves form tiny bubbles due to energy imparted to the blood during closure of the valve.¹⁶

Distinguishing solid from gaseous emboli

Although small gas bubbles and larger solid emboli theoretically produce similar signal intensities, signals with MEBRs exceeding 40 dB can normally be confidently assumed to be gaseous (Fig. 12). Gaseous emboli from cardiac sources produce signals with MEBRs up to ~60 dB, but intensities lower than 10 dB are rare, since bubbles of less than 4 µm diameter tend to dissolve before reaching the brain.¹⁵

Differences between the scattering properties of solid and gaseous emboli can be used as the basis for distinguishing between them (Fig. 17). In studies examining large populations of embolic signals, a statistical approach to estimating the proportion of solid and gas emboli may be appropriate (Fig. 18). The development of reliable methods for estimating embolus size and composition from specific embolic signals is still ongoing.^{20–23}

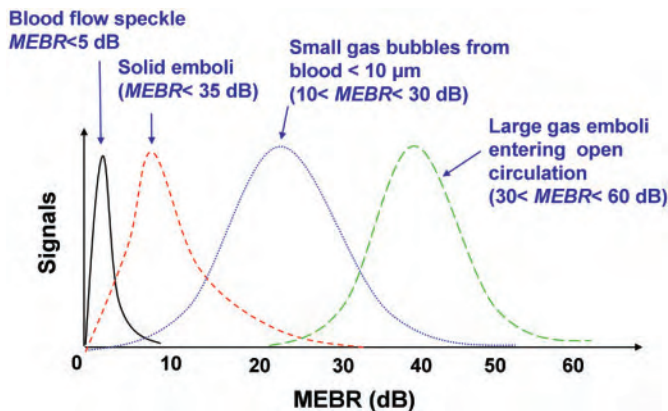


Figure 17. Schematic diagram of the intensity distributions of different sources of embolic signal.

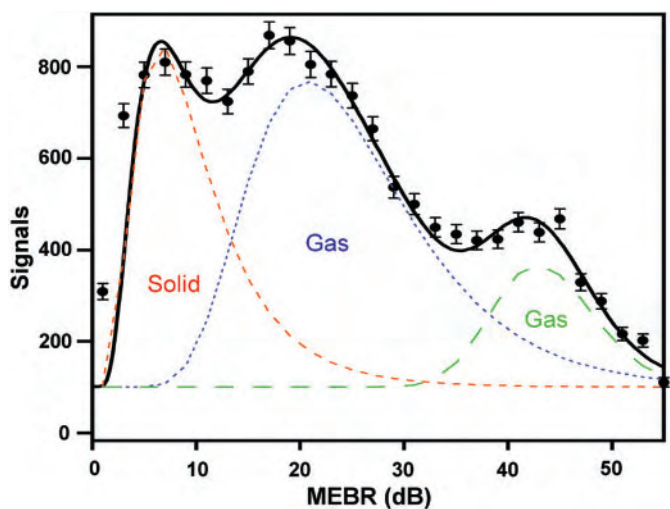


Figure 18. Statistical separation of solid and gaseous emboli for 10 cardiac surgery patients. Numbers of emboli in each population can be estimated from the areas under the curves.

Frequency modulation

Gas emboli are more likely to experience changes in velocity than solid emboli. This can be observed in the audio signal and sonogram as frequency modulation (Fig. 19). It is hypothesized that gas bubbles exhibit stronger frequency modulation than solids, because their trajectories are erratic and easily affected by pressure from the ultrasound beam.²²

Frequency response

Small gas bubbles are more 'point-like' than solid emboli and are therefore better Rayleigh scatterers (see Fig. 8). By increasing the frequency of the ultrasound beam (e.g. from 2 to 2.5 MHz), the intensity of Rayleigh scattering is greatly increased. This can be used to help to distinguish large solid emboli from 'point-like' gaseous emboli. Since bubbles of different diameters resonate at different frequencies, by changing the ultrasound frequency it may be possible to estimate bubble sizes by detecting resonance effects.²¹

Clinical Embolus Detection

Routine detection of embolic signals is time-consuming and costly due to a heavy reliance on human observers. Psychoacoustics tests based on presenting simulated embolic signals to healthy volunteers, suggest that many embolic signals are barely detectable by the human auditory system.²⁴ Detection of emboli starts to be limited by psychoacoustics effects for signals with MEBRs <14 dB. These limitations are exacerbated by the noisy and distracting environment of the operating theatre or recovery room, which reduces detection by a further ~25% compared with ideal conditions (Fig. 20).²⁵

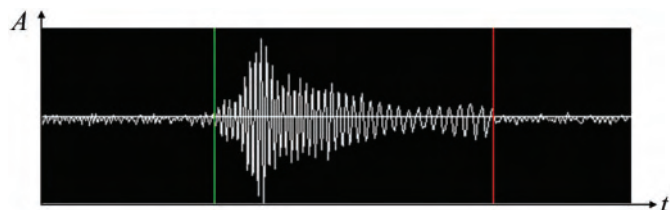


Figure 19. Appearance of frequency modulation.

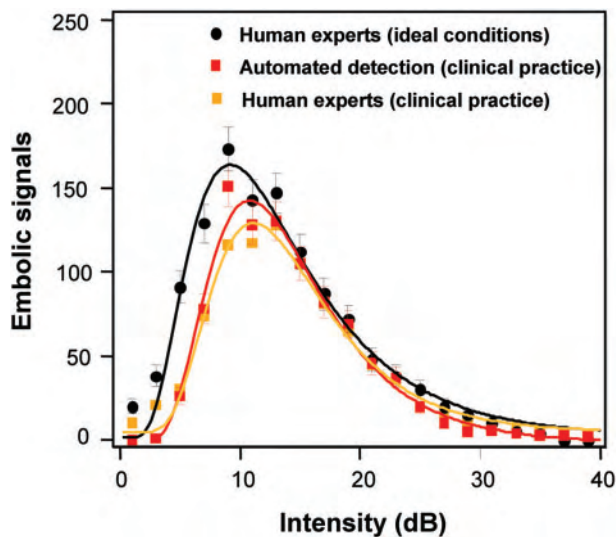


Figure 20. Distributions measured under clinical conditions contain 25% fewer signals than under ideal conditions, due to an increase of the threshold of detection by ~2 dB.²⁵

Automated detection

A more practical and potentially more reliable method of detecting embolic signals is using automated embolus detection. A number of automated detection systems have been recently been developed based on a range of signal analysis techniques.^{20,21,26–29}

Discrimination between embolic signals and artefacts may be achieved by simultaneous monitoring of multiple sample depths (Fig. 21). (Machines designed to probe more than one depth are called ‘multi-gate’ Doppler devices.) Differentiation between emboli and artefacts is based on the principle that embolic signals appear sequentially in the insonated artery, while artefacts (such as coughing, speech, or probe movement) are observed at all depths simultaneously, regardless of the position of the insonation volume.

Automated systems are currently being tested for a range of clinical applications,^{25,28,29} however, assessment of the performance of automated systems is complicated by the absence of a true ‘gold-standard’. No systems have yet been unanimously agreed to be suitable for routine clinical use. Automated detection enables extended analysis of embolic signal properties, which will be essential for deducing further information about embolus size and composition. Automated detection devices also have potential to act as a ‘standardized observer’. This may prove useful for performing comparative studies or as a quality control measure during large multi-centre trials.

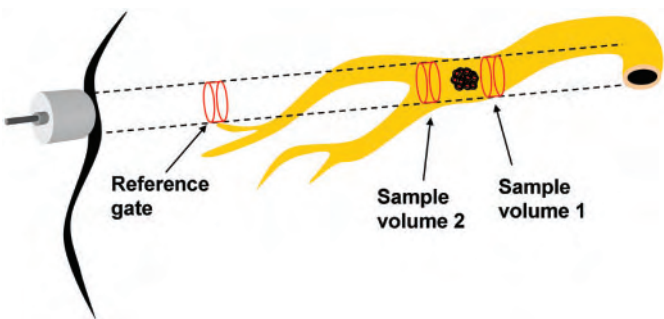


Figure 21. Emboli pass sequentially through sample volumes 1 and 2, but are not observed at the reference gate positioned outside of the artery. Artefacts are observed at all depths simultaneously including the reference gate.

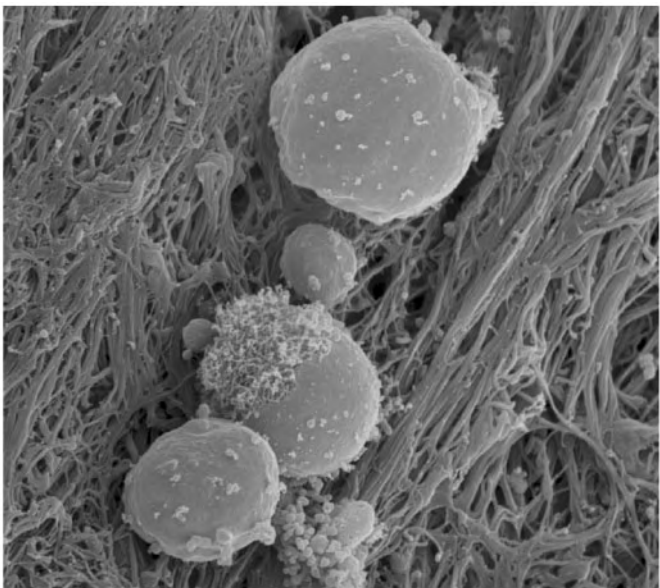


Figure 22. Scanning electron microscope image of targeted microbubbles (immunobubbles) adhering to the surface of a thrombus.

Future Directions

Targeted microbubbles

Antibody-coated ultrasound contrast bubbles (immunobubbles) have recently been engineered to selectively adhere to specific types of plaque and thrombus (Fig. 22). Injection of immunobubbles (e.g. into the carotid artery) could be useful in for distinguishing if embolization is occurring from thrombus or from plaque. Due to their high acoustic impedance, bubbles enhance the detection of weakly scattering emboli. In future, they may also provide a means of delivering encapsulated pharmaceuticals, labelling emboli using radioactive tracers, or disintegrating thrombus using ultrasonic resonance.

Inhalation of gases

It is possible to alter the mixture of gases in the blood by asking patients to inhale oxygen or by flooding the operative area with fast-dissolving gases such as carbon dioxide. This alters the properties of gaseous emboli, which can help to reduce the number and average size of gas bubbles reaching the brain. This can also be used to deduce the source of embolization and distinguish whether emboli are mainly solid or gaseous.^{16,19}

Adaptive focusing

The skull causes severe distortion of the ultrasound beam, which has potential to be overcome by a technique known as adaptive focusing.³⁰ By compensating for scattering by the skull when choosing the form of the incident ultrasound, it becomes possible to significantly reduce the effects of distortion. This would enable more uniform insonation of arteries and simplify the analysis of Doppler embolic signal data.

Computer simulations of embolic load

Information about embolus composition, size and prevalence gained from TCD monitoring could be used to provide estimates of embolic load. Recent breakthroughs in characterization of vessel sizes and the mapping of complex arterial networks³¹ makes it possible to incorporate quantitative descriptions of the cerebral vasculature into models investigating regulation of blood-flow, oxygen transport and embolization.

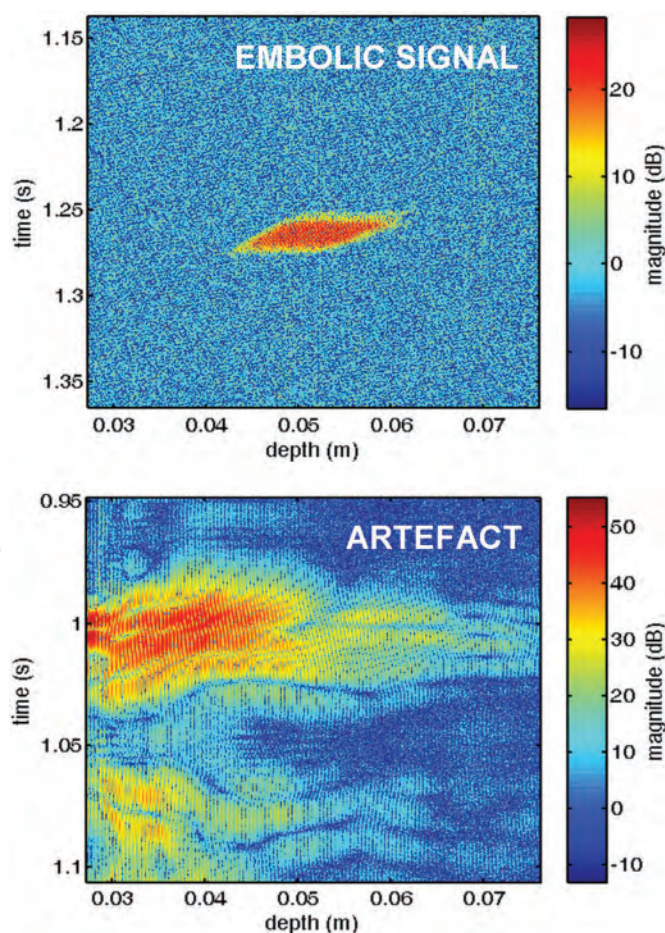


Figure 23. RF data is plotted as time on the y-axis and depth on the x-axis. Embolic signals occur over a finite range of depths (top panel), while artefacts produce more disperse RF characteristics (bottom panel).³² Changes in the trajectories of emboli can also be more clearly visualized using RF data.³³

RF signal analysis

Improved visualization of embolus trajectory and better identification of emboli, can be achieved by recording and analysing the raw RF signal coming directly from the transducer (Fig. 23). Currently, a two second recording of the RF signal is computationally expensive to store and analyse in real time, so RF data analysis is usually reserved for research studies.^{32,33}

Conclusions

In understanding embolic stroke, the detection and characterization of emboli is an important and rapidly developing field of research. Although the extension of embolus detection techniques to routine clinical use remains in its infancy, I hope that this article has demonstrated a wide range of interesting problems, and promising applications in the detection and characterization of cerebral emboli using transcranial Doppler ultrasound.

Acknowledgements

My thanks go to my friends and colleagues, especially Lorna Sweetman (for supplying data for Fig. 2), David Evans (Figs 12), Matthew Martin (Fig. 22) and Joanne Cowe (Fig. 23).

References

1. Lopez AD, Murray CJL. The global burden of disease. *Nature Med* 1998;4:1241–1243.
2. Babikian VL, Wechsler LR (Eds) *Transcranial Doppler Ultrasonography*. Butterworth Heinemann, Boston, 1999.
3. Markus H. Transcranial Doppler detection of circulating cerebral emboli. A review. *Stroke* 1993;24:1246–1250.
4. Droste DW, Ringelstein EB. Review: detection of high intensity transient signals (HITS): how and why? *Eur J Ultrasound* 1998;7:23–29.
5. Doppler C, quoted by White DN. Johann Christian Doppler and his effects—a brief history. *Ultrasound Med Biol* 1982;8:583–591.
6. Buys Ballot CHD. Bedrog van het gehoororgaan in het bepalen van de hoogte van een waargenomen toon. *Caecilia. Algemeen Miz Tijdschr Ned* 1845; Tweede jaargang, 7:78–81.
7. Evans DH, McDicken WN. *Doppler ultrasound physics, instrumentation and signal processing*, 2nd edn. John Wiley, Chichester, 2000.
8. John William Strutt (Lord Rayleigh). *The Theory of Sound*, Vol. II, 2nd edn. Macmillan, London (1896) [reprinted Dover, New York, 1945].
9. Jarquin-Valdiva AA, Mitsky NN. The horizontal angle of the middle cerebral artery from the middle TCD temporal window. *J Diagn Med Sonogr* 2004;20:16–19.
10. Droste DW, Markus HS, Nassiri D, Brown MM. The effect of velocity on the appearance of embolic signals studied in transcranial Doppler models. *Stroke* 1994;25:986–991.
11. Basic identification criteria of Doppler microembolic signals consensus committee of the 9th International Cerebral Haemodynamics Symposium. *Stroke*, 1995;26:1123.
12. Evans DH. Microembolic signals, in: Babikian VL, Wechsler LR (Eds) *Transcranial Doppler Ultrasonography*. Butterworth Heinemann, Boston, 1999.
13. Moehring MA, Klepper JR. Pulse Doppler ultrasound detection, characterisation and size estimation of emboli in flowing blood. *IEEE Trans Biomed Eng* 1994;41:35–44.
14. Evans DH. Ultrasonic detection of cerebral emboli, in: Yuhas DE, Schneider SC, (Eds) *Proceedings of the 2003 IEEE Ultrasonics Symposium*. Piscataway: IEEE. 2003;316–326.
15. Bucerius J, Gummert JF, Borger MA, *et al*. Stroke after cardiac surgery: a risk factor analysis of 16,184 consecutive adult patients. *Ann Thorac Surg* 2003;75:472–478.
16. Kaps M, Hansen J, Weiher M, *et al*. Clinically silent microemboli in patients with artificial prosthetic aortic valves are predominantly gaseous and not solid. *Stroke* 1997;28:322–325.
17. Angell EL, Evans DH. Limits of uncertainty in measured values of embolus-to-blood ratio due to Doppler sample volume shape and location. *Ultrasound Med Biol* 2003;29:1037–1044.
18. Chung EML, Fan L, Naylor AR, Evans DH. Characteristics of Doppler embolic signals observed following carotid endarterectomy. *Ultrasound Med Biol* 2006;32:1011–1023.
19. Barak M, Katz Y. Microbubbles: pathophysiology and clinical implications. *Chest* 2005;128:2918–2932.
20. Russell D, Brucher R. Online automatic discrimination between solid and gaseous cerebral microemboli with the first multifrequency transcranial Doppler. *Stroke* 2002;33:1975–80.
21. Buckley JC, Knaus DA, Alvarenga DL, *et al*. Dual-frequency ultrasound for detecting and sizing bubbles. *Acta Astronaut* 2005;56:1041–1047.
22. Smith JL, Evans DH, Naylor AR. Analysis of the frequency modulation present in Doppler ultrasound signals may allow differentiation between particulate and gaseous emboli. *Ultrasound Med Biol* 1997;23:727–734.
23. Evans DH. Embolus differentiation using multifrequency transcranial Doppler. *Stroke* 2006;37:1641.
24. Chung EML, Fan L, Degg C, Evans DH. Detection of Doppler embolic signals: psychoacoustic considerations. *Ultrasound Med Biol* 2005;31:1177–1184.

25. Chung EML, Fan L, Naylor AR, Evans DH. Impact of clinical environment on embolus detection; a comparison of automated and manual detection of embolic signals. Cerebrovascular diseases. (In press).

26. Dittrich R, Ritter MA, Droste DW. Microembolus detection by transcranial Doppler sonography. [Eur J Ultrasound 2002;16:21–30.](#)

27. Fan L, Evans DH, Naylor AR, Tortoli P. Real-time identification and archiving of micro-embolic Doppler signals using a knowledge-based SP system. [Med Biol Eng Comput 2004;42:193–200.](#)

28. Markus HS, Punter M. Can transcranial Doppler discriminate between solid and gaseous microemboli? Assessment of a dual-frequency transducer system. [Stroke 2005;36:1731–1734.](#)

29. Cullinane M, Kaposzta Z, Reihill S, Markus HS. Online automated detection of cerebral embolic signals from a variety of embolic sources. [Ultrasound Med Biol 2002;28:1271–1277.](#)

30. Aubry JF, Tanter M, Pernot M, *et al.* Experimental demonstration of non-invasive trans-skull adaptive focussing based on prior computed tomography scans. [J Acoust Soc Am 2003;113:84–93.](#)

31. Cassot F, Lauwers F, Fouard C, *et al.* A novel three-dimensional computer assisted method for a quantitative study of microvascular networks of the human cerebral cortex. *Microcirculation* 2006;13:1.

32. Cowe J, Gittins J, Naylor AR, Evans DH. RF signals provide additional information on embolic events recorded during TCD monitoring. [Ultrasound Med Biol 2005;31:613–623.](#)

33. Mess WH, Willigers JM, Ledoux LA, *et al.* Microembolic signal description: a reappraisal based on a customized digital post-processing system. [Ultrasound Med Biol 2002;28:1447–1455.](#)